FAILURE OF A BUNDLE OF CERAMIC FIBRES IN A CMC

R. Paar and J.L. Vallés *

The failure process of a bundle of reinforcing fibers in a unidirectional ceramic matrix composite is studied. By substructuring the embedded fibres into short elements and using a shear lag model to evaluate the stress profile, the stress - strain plots for a composite with matrix crack saturation as well as the local distribution of fibre failures are calculated. Results of a simulation using constituent properties of a real material are presented.

INTRODUCTION

Continuous fibre-reinforced ceramic matrix composites (CMCs) are promising candidates for high temperature structural applications, where reliability is a major issue, because unlike monolithic ceramics they show a strong non-linear behaviour which is due to the activation of new damage mechanisms.

In this work a unidirectionally reinforced CMC is considered, which is loaded parallel to the fibres axis. Since the failure strain of the matrix is usually lower than that of the fibres, progressive matrix microcracking leads to a reduction of the matrix stresses, until saturation of matrix cracking is reached. The composite then consists of a series of matrix blocks connected by the bundle of continuous fibres. Due to the periodicity in the stress profile along the fibres resulting from the matrix crack distribution, the reinforcing bundle can be considered as a chain of shorter bundles, each associated to a matrix block. The failure of the CMC results from the process of fibre failure. The strength of a bundle of loose fibres has been described analytically by

* Institute for Advanced Materials, Joint Research Centre, European Commission, P.O.Box 2, 1755 ZG Petten, The Netherlands

Daniels (1), but when the bundle is surrounded by a matrix the study is more complex.

In our modelling approach, following the weakest link theory the fibres are subdivided along the axis into small elements, and each element is provided with a randomly generated breaking stress, chosen from a given strength distribution which mimics the flaw population. During the loading process in a tensile test, the local stress in the different fibre segments can be calculated using a shear-lag model. Then, where the local stress first exceeds the strength of a fibre element the fibre is considered to fail. The stress profile is subsequently updated according to the new boundary conditions and the load is redistributed among the fibres. In this way the process of fibre failure can be monitored.

MODELLING APPROACH

In accordance with the weakest link theory a fibre of length l that survives a uniform tensile stress σ with probability P can be considered as a series of n elements with length $l_j = l/n$, each surviving the stress σ with a higher probability P_j. Using a Weibull distribution these probabilities are

$$P = \left(P_j\right)^n = \exp\left(-\frac{l_j \cdot n}{l_0} \cdot \left(\frac{\sigma}{\sigma_0}\right)^m\right), \qquad (1)$$

where σ_0 and m are the parameters of the distribution and l_0 is a normalising length. For a bundle between two matrix cracks having N brittle fibres each with n elements (see figure 1), using equation (1) an array of $N \times n$ strengths or breaking stresses is sampled.

In our simulation we assume that the saturation of matrix cracking is reached before any fibre has failed. In order to calculate the fibre stress distribution a series of coaxial cylindrical elements is used, in which the fibre is embedded in the matrix blocks between matrix cracks. In any of these cylindrical elements, sliding conditions at the interface between fibre and matrix are assumed, and the shear along the interface is governed by a Coulomb friction law involving the friction coefficient μ, the radial clamping stress σ_c and the radial stress caused by the Poisson effect, σ_i. Using the approach followed by Takaku and Arridge (2) and Hsueh (3) to study fibre pull-out, the relation between the axial stress σ_f and the interfacial shear stress τ_i is given by

$$\frac{d\sigma_f}{dx} = -\frac{2}{r_f}\tau_i, \qquad (2)$$

where $\tau_i = \mu\,(\sigma_i + \sigma_c)$, and the stress profile can be obtained analytically.

If n is large, the stress is assumed to be constant in each fibre element, and thus the stress profile along the whole fibre length is approximated by a step function. The applied stress, understood as the one applied on an individual fibre at the edge of a matrix block, which is necessary to break the fibre at each element, *i.e.* which gives a local stress equal to the strength of the element, is then calculated. The smallest of these stresses for each fibre is the critical applied stress, since the fibre will break at this applied stress and at the corresponding element. Sorting these fibre applied stresses in ascending order gives the sequence in which the fibres will break.

If the matrix is much stiffer than the fibres it can be assumed that a fibre failure does not locally influence the stress state in neighbouring elements of other fibres. This means that the local distribution of fibre failures only depends on the parameters of the Weibull distribution and on the stress profile along the fibre axis. Further, since the broken fibres can still carry a small load which depends on the position where the failure occurred, because of interfacial load transfer, these loads are taken into account when computing the total composite applied stress in order to construct the stress-strain curve.

RESULTS

A simulation has been carried out for a bundle of N = 5000 and n = 500. The thermo-elastical material properties were taken from a real CMC and are given in table 1. Other parameter values used were a fibre radius r_f = 5.5 μm, a fibre volume fraction V_f = 0.35, an interfacial friction coefficient μ = 0.06 and a drop from manufacturing temperature ΔT = -1000 K. The parameters of the strength distribution are m = 4, l_0 = 50 mm and σ_0 = 1.1 GPa.

TABLE 1- Material properties in the axial and radial directions

	E_{ax} (GPa)	E_{rad} (GPa)	ν_{ax}	ν_{rad}	α_{ax} ($10^{-6}K^{-1}$)	α_{rad} ($10^{-6}K^{-1}$)
Matrix (Si_3N_4)	300	300	0.27	0.27	-0.9	11
Fibres (C)	40	140	0.12	0.42	3.6	3.6

The stress profiles along the fibre axis for different applied stresses are plotted in figure 2. Prior to loading, the fibre is subjected to a residual compressive stress σ_{res} caused by the cooling down after processing, except at the block edges, where the fibre stress goes to zero. When the fibre is increasingly loaded, the local stresses in the fibre grow, as well as the fraction of the fibre which is under tensile stress. When the applied stress reaches a threshold value, there is a complete radial detachment between fibre and matrix, and the fibre is subjected to a uniform stress state.

In figure 3 the (stress, strain)-states corresponding to the fibre failures in two different simulations, equivalent to strain-controlled tensile tests on a CMC unloaded after matrix crack saturation, are plotted together with the evolution of the fraction of broken fibres. Curve *a* is the stress *versus* strain plot in the case of a fibre bundle embedded in a matrix block for ΔT=-1000K. Curve *b* corresponds to ΔT = 0K, *i.e.* a case with total detachment, and shows the behaviour of a loose fibre bundle, in agreement with the analytical solution. Curves *c* and *d* are the fraction of broken fibres *versus* strain for ΔT= -1000K and ΔT = 0K respectively. As expected from a Weibull distribution of strengths, this fraction grows steeply in a small range of strains.

The local distribution of fibre failures is presented in figure 4, where the position of the breaking flaw is plotted versus the fibre rank in order of failure. As expected, the first fibres fail near the matrix crack, because only this part is under tension, whilst the rest of the fibre is still under residual compressive stress. As the applied stress increases the fibres break on average deeper inside the matrix block. Since the fibre stress is still highest near the matrix crack it could be expected that many fibres keep breaking there, but the figure shows the contrary, because the fibres which were weak in that region are already broken. When the applied stress causing total detachment is reached, the local stress becomes uniform inside the block and the fibre failure positions are also uniformly distributed. This behaviour can also be illustrated by computing the statistical parameters of the distribution of fibre failures in figure 4 at different stages during the process. A distribution of pull-out lengths can easily be obtained from the positions of the breaking flaws, as will be reported elsewhere.

ACKNOWLEDGEMENTS

This work has been performed within the Specific Research and Development Programme of the European Commission. We thank C. Olivier for providing experimental data and M. Steen for helpful discussions.

REFERENCES

(1) Daniels H.E., Proc. R. Soc. London A, Vol. 183, 1945, pp 405-435

(2) Takaku, A. and Arridge, R.G.C., J. Phys. D Appl. Phys., Vol. 6, 1973, pp. 2038-2047.

(3) Hsueh, C.-H., J. Mater. Sci., Vol. 25, 1990, pp. 811-817

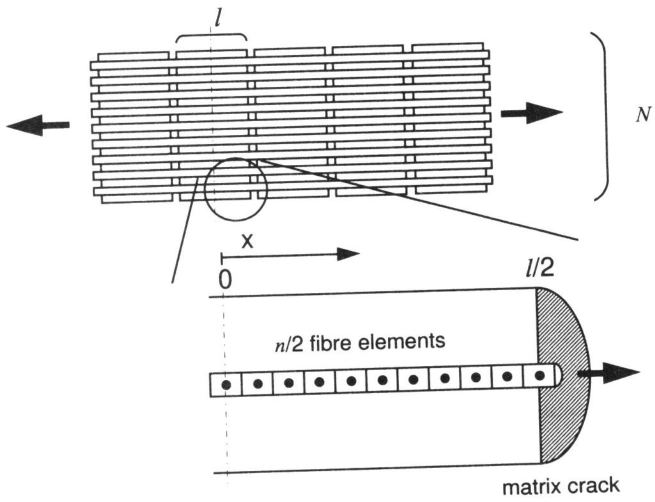

Figure 1. Coaxial cylinder model used in the simulation.

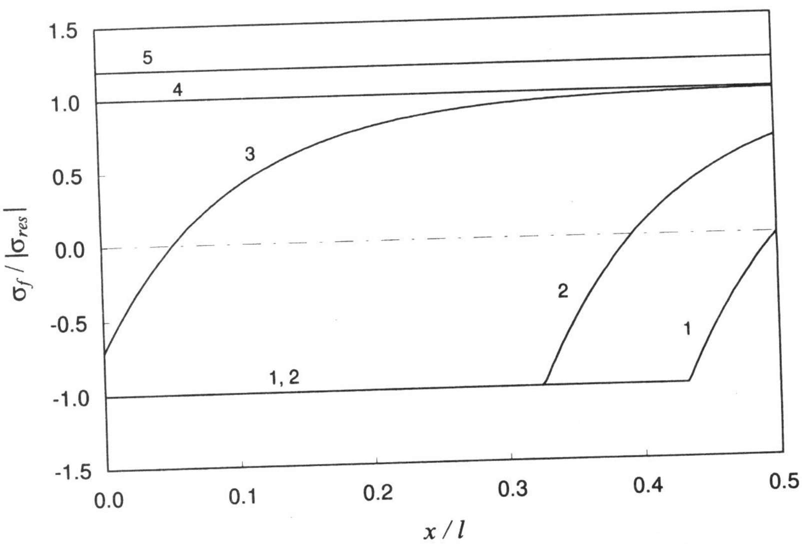

Figure 2. Stress distribution along the fibre axis for different applied stresses.

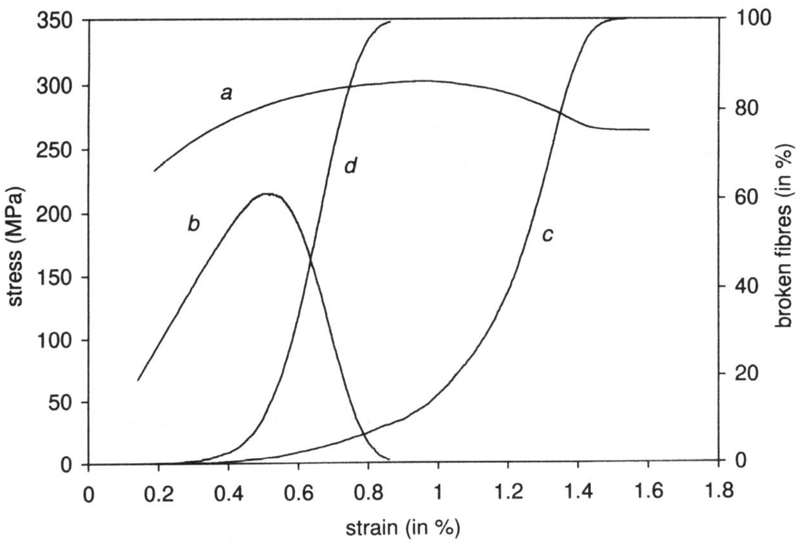

Figure 3. Stress-strain plot and evolution of the fraction of broken fibres.

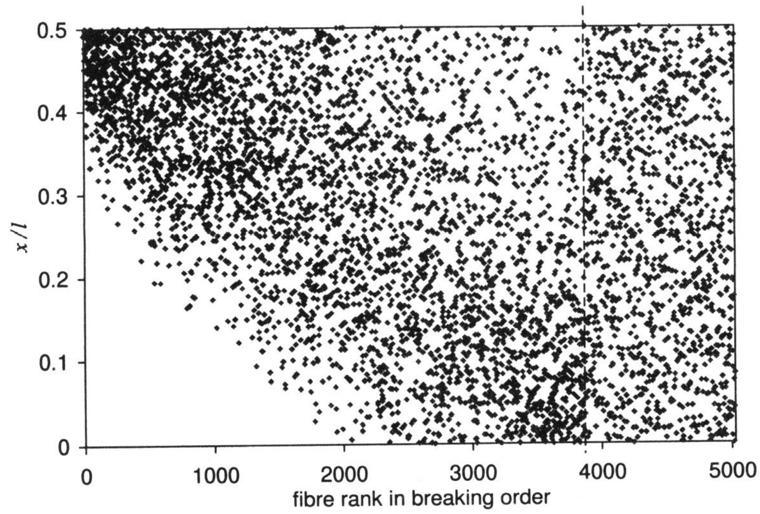

Figure 4. Local distribution of fibre failures during a simulated tensile test for ΔT = -1000K. The dashed line shows the attainment of total detachment.